

CONTRIBUTION NO. 1286 FROM THE CENTRAL RESEARCH DEPARTMENT, EXPERIMENTAL STATION,  
E. I. DU PONT DE NEMOURS AND COMPANY, WILMINGTON, DELAWARE 19898

## Chemistry of Boranes. XXVIII.<sup>1</sup> New Polyhedral Borane Anions, $B_9H_9^{2-}$ , $B_8H_8^-$ , and $B_7H_7^{2-}$

By F. KLANBERG, D. R. EATON, L. J. GUGGENBERGER, AND E. L. MUETTERTIES

Received January 30, 1967

Air oxidation of  $B_9H_9^{2-}$  ion under carefully prescribed solution conditions generates a series of polyhedral ions which include the known  $B_6H_6^{2-}$  ion and the previously unknown  $B_8H_8^{2-}$  and  $B_7H_7^{2-}$  ions. An intermediate in this oxidation is a paramagnetic species which has been assigned the composition  $B_8H_8^{\cdot -}$ . This ion-radical provides the first really definitive information regarding delocalization of electrons in polyhedral cages. The structure of the ion-radical is not established; however, on the esr time scale spectral analysis indicates that all boron and hydrogen atoms are equivalent and equally coupled with the odd electron. The structure of  $B_8H_8^{2-}$  in the tetraamminezinc salt has been shown to be a slightly distorted  $D_{2d}$  dodecahedron that is strikingly similar to the  $B_8Cl_8$  geometry. The solid-state structure of  $B_7H_7^{2-}$  has not yet been determined; however, nmr data suggest that this ion has  $D_{5h}$  symmetry (pentagonal bipyramidal geometry) or a closely related  $C_2$  symmetry in solution. The chemical reactivity of the  $B_8H_8^{2-}$  ion is comparable to that of  $B_9H_9^{2-}$  ion, and thermal stability is similar in that the cesium salt is stable to at least 600°. The  $B_7H_7^{2-}$  ion possesses the highest reactivity of all the polyhedral borane anions from  $B_6H_6^{2-}$  through  $B_{12}H_{12}^{2-}$ .

### Introduction

We have previously<sup>1</sup> extended the series of triangulated coordination polyhedra of binary boron hydrides to the polyhedral anions  $B_9H_9^{2-}$  and  $B_{11}H_{11}^{2-}$ . In this paper we report the isolation and characterization of new members of the polyhedral ion series, namely,  $B_8H_8^{2-}$ ,  $B_8H_8^-$ , and  $B_7H_7^{2-}$ . With the structural information now available for this series ranging from  $B_6$  through  $B_{12}$ , all of the polyhedral borane anions can be characterized as triangulated polyhedra. Previously anticipated geometries in the  $B_8$  system with some nontriangulated faces, such as the square antiprism and the symmetrically bicapped trigonal prism, appear to be significantly higher energy geometries for this particular polyhedral borane. The series of polyhedral borane anions is now complete<sup>2</sup> from the  $B_6H_6^{2-}$  ion through the  $B_{12}H_{12}^{2-}$  ion.

In the analogous carborane system triangulated polyhedra should prevail, too. Thus in the  $B_6C_2$  framework, the geometry will probably closely approximate that of a dodecahedron although there may be some significant distortion due to  $C^+-C^+$  repulsions.<sup>3-5</sup>

The neutral  $B_8Cl_8$  structure established some time ago<sup>6</sup> has been described variously in the literature as a distorted dodecahedron and a distorted square antiprism, but Pawley's refinement of the data indicates that the structure more closely approximates that of the dodecahedron and is strikingly similar to  $B_8H_8^{2-}$  geometry.

**Synthesis.**—Dissolution of the hydrated sodium salt<sup>1</sup> of  $B_9H_9^{2-}$  in aliphatic ethers such as tetrahydrofuran or dimethoxyethane is accompanied by a red coloration if carried out in the presence of air. Prolonged exposure of such solutions<sup>7</sup> to air at temperatures above 25° leads to an intensification of the red color initially, but the intensity gradually diminishes and a milky white solid, presumably the sodium salt of  $B_8H_8^{2-}$  ion, begins to precipitate. The addition of water and large cations to the reaction mixture provides for the isolation of the anion  $B_8H_8^{2-}$  in substantial conversions

(3) R. E. Williams and F. J. Gerhart, *J. Am. Chem. Soc.*, **87**, 3513 (1965), favor the dodecahedron.

(4) F. N. Tebbe, P. M. Garrett, D. C. Young, and M. F. Hawthorne, *ibid.*, **88**, 609 (1966), proposed a square antiprismatic  $B_8C_2$  framework.

(5) W. N. Lipscomb, *Science*, **153**, 373 (1966), has proposed an intermediate structure based on distortion of the square antiprismatic structure for  $B_8C_2$  carboranes in which the distances between the *trans* carbon atoms are elongated accompanied by a shortening of the *trans* boron atoms on one of the square faces.

(6) (a) M. Atoji and W. N. Lipscomb, *J. Chem. Phys.*, **31**, 601 (1959); (b) R. A. Jacobson and W. N. Lipscomb, *ibid.*, **31**, 605 (1959); (c) G. S. Pawley, *Acta Cryst.*, **20**, 631 (1966).

(7) If the red solution in tetrahydrofuran is cooled to 0° immediately after preparation, most of the  $B_9H_9^{2-}$  anion present separates out as colorless needles of  $Na_2B_9H_9 \cdot 4H_2O$ .

(1) Paper XXVII: F. Klanberg and E. L. Muetterties, *Inorg. Chem.*, **5**, 1955 (1966).

(2) For more detailed references to polyhedral boranes and carboranes, see the following reviews: (a) E. L. Muetterties and W. H. Knoth, *Chem. Eng. News*, **44** (19), 88 (May 9, 1966); (b) W. H. Knoth and E. L. Muetterties, "Polyhedral Borane Chemistry," to be published in "Molecular Hydrides," J. A. Ibers, Ed., Academic Press Inc., New York, N. Y.; (c) M. F. Hawthorne, *Endeavour*, **25**, 146 (1966).

(approximately 50%). For optimum conversions to this ion it is critical to stop the oxidation when the red color has essentially disappeared. If oxidation is continued beyond this point, small amounts of other borane ions such as  $B_3H_8^-$ ,  $B_6H_6^{2-}$ ,  $B_{10}H_{10}^{2-}$ , and  $B_7H_7^{2-}$  as well as boric acid can be detected and isolated.

The formation of the red color during oxidation of  $B_9H_9^{2-}$  is accompanied by the appearance of a strong and complex esr spectrum which has been assigned to the radical anion  $B_8H_8^-$  (*vide infra*), although it has not been rigorously established whether the color itself is associated with the ion-radical. Qualitative observations on the lifetimes of the colored species and the esr signal indicate they are similar and are representative of the same species. The equilibrium between the paramagnetic  $B_8$  ion-radical and the colorless diamagnetic  $B_8$  dianion,  $e^- + B_8H_8^- \rightleftharpoons B_8H_8^{2-}$ , appears to lie far on the right. The position of the equilibrium and its rapid attainment complicate the isolation of pure salts of the monovalent anion. Salts of  $B_8H_8^-$  have been isolated only in admixture with salts of the  $B_8H_8^{2-}$  ion.

The oxidation of the sodium salt of  $B_8H_8^{2-}$  under conditions similar to those described above for the oxidation of  $B_9H_9^{2-}$  generates the ion  $B_7H_7^{2-}$  in low and somewhat erratic yields. The principal other product in this degradation is the ion  $B_6H_6^{2-}$ , but small amounts of other ions such as  $B_{10}H_{10}^{2-}$ ,  $B_{12}H_{12}^{2-}$ , and  $BH_4^-$  are also formed in the process.

**Chemical Properties of  $B_7H_7^{2-}$  and  $B_8H_8^{2-}$ .**—The  $B_7H_7^{2-}$  ion is the least stable polyhedral ion known to date. We have found it difficult to isolate significant quantities of its salts, which has complicated a rigorous characterization of this particular ion. On dissolution of the  $B_7H_7^{2-}$  ion in water, there is an immediate, slow evolution of hydrogen. Although lacking quantitative data on hydrolysis rate, we can say without equivocation that  $B_7H_7^{2-}$  is the most hydrolytically unstable polyhedral ion. This hydrolytic instability is at least an order of magnitude greater than that of the ions of intermediate hydrolytic stability such as  $B_6H_6^{2-}$ ,  $B_8H_8^{2-}$ , and  $B_9H_9^{2-}$ . The low hydrolytic stability of  $B_7H_7^{2-}$  is readily rationalized on the basis of the high charge density as well as the relative localization of charge within the polyhedron (relative to the more symmetrical polyhedral ions).

The hydrolytic stability of the  $B_8H_8^{2-}$  ion is comparable to that of the analogous ions  $B_6H_6^{2-}$  and  $B_9H_9^{2-}$ . The anion is unaffected by base but it is rapidly degraded by hydronium ions in aqueous solution giving rise to boric acid and hydrogen. Oxidizing agents such as iron(III), mercury(II), and copper(II) accelerate the decomposition.

Consistent with the fact that  $B_8H_8^{2-}$  is subject to air oxidation, we find that it is also oxidized by ions such as silver ion, a property atypical of divalent polyhedral borane anions. Silver salts of  $B_6H_6^{2-}$  and  $B_9H_9^{2-}$  have been isolated, although these salts have a relatively high thermal reactivity and are photosensitive.<sup>1,8</sup> The thermal stability of certain salts of

$B_8H_8^{2-}$  is quite high. There was no evidence of degradation of the cesium salt after a 1-hr exposure at 600° in an evacuated sealed tube. Thus this ion has about the same thermal stability as  $B_6H_6^{2-}$ ,  $B_9H_9^{2-}$ , and  $B_{10}H_{10}^{2-}$ .

Polarographic studies of the divalent  $B_6$ ,  $B_8$ , and  $B_9$  anions under strictly identical conditions established the oxidative stability of all these ions to be quite comparable. The half-wave potentials lie very close to the potential of the reference electrode (sce).

In alkaline solution the  $B_8H_8^{2-}$  ion can be brominated without extensive degradation to give the hexabromo derivative, the  $B_8Br_6H_2^{2-}$  ion. In contrast to the previously described halo anions of the  $B_9$  polyhedron, namely,  $B_9Cl_3H^2-$  and  $B_9Br_6H_3^{2-}$ ,<sup>1,2b</sup> the hexabromo  $B_8$  anion is stable toward acid degradation. It is perhaps dangerous to speculate on this difference in behavior; however, this stability, whether it is kinetic or thermodynamic in nature, might reside in the fact that the boron atoms in the  $B_8$  system do not significantly differ in environment or charge density, whereas in the  $B_9$  system there are two distinct boron atom environments in the symmetrically tricapped trigonal prismatic geometry. The three capped boron atoms in the latter structure are only five-coordinate and may provide through their lower coordination number and also higher charge density sites more susceptible to electrophilic attack and degradation.

**Structural Characterization of the New Anions.**—The anion  $B_7H_7^{2-}$  shows in solution a two-line  $B^{11}$  nmr pattern of relative intensities 5 and 2, each absorption line being split into a doublet due to BH spin-spin coupling (Figure 1). This establishes a minimum of two boron atom environments, and strictly speaking this is the most that can be said about the structure of this ion in solution. These data are consistent with pentagonal bipyramidal geometry ( $D_{5h}$  symmetry), at least for the average configuration within the nmr time scale (see, however, the theoretical discussion of the  $B_7$  case below). To date we have no structural data for this anion in its crystalline salts. We would expect, however, at the very least that there will be some distortion, even though it may be minimal. Moreover, in the solid state packing forces may lead to further distortion from the idealized geometries. The related carborane<sup>9</sup>  $B_5C_2H_7$  has near pentagonal bipyramidal geometry in the gaseous state.

The molecular and crystal structures of  $Zn(NH_3)_4 \cdot B_8H_8$  have been determined by X-ray diffraction techniques. Crystals of  $Zn(NH_3)_4 \cdot B_8H_8$  are tetragonal with cell parameters  $a = 7.50 \pm 0.02$  Å and  $c = 10.78 \pm 0.03$  Å. The space group is  $P4_2/nmc$  and there are two formula units per unit cell. Three-dimensional data were collected on a Picker diffractometer using molybdenum radiation.

The boron atom positions were determined from an electron density map with the phases determined by the

(8) J. L. Boone, *J. Am. Chem. Soc.*, **86**, 5036 (1964).

(9) T. Onak, G. B. Dunks, R. A. Beaudet, and R. L. Poynter, *ibid.*, **88**, 4622 (1966).

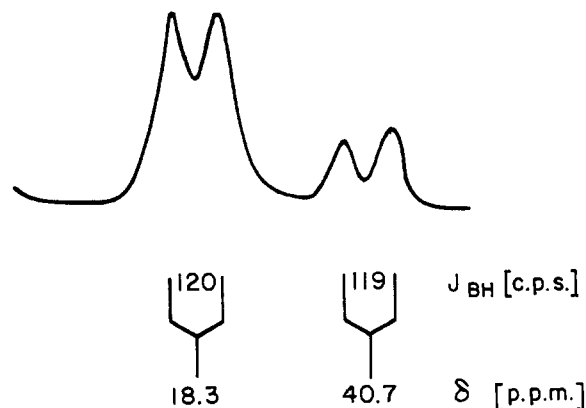


Figure 1.— $B^{11}$  nmr spectrum of  $Cs_2B_7H_7$  in  $H_2O$  at 19.3 Mc; external reference  $B(OCH_3)_3$ .

Zn and N atom contributions. The discrepancy factor  $R = \Sigma ||F_o| - |F_c|| / \Sigma |F_o|$  is 0.10 at this point in the refinement. No attempt has been made as yet to locate any of the hydrogen atom positions.

The structure of the  $B_8$  polyhedron is illustrated in Figure 2. The point symmetry of this polyhedron is  $D_{2d}$ ; the  $S_4$  axis passes through the midpoints of  $B(1)-B(2)$  and  $B(7)-B(8)$ , one of the  $C_2$  axes passes through the midpoints of  $B(3)-B(5)$  and  $B(4)-B(6)$ , and one of dihedral mirror planes contains the atoms  $B(3)-B(4)-B(7)-B(8)$ . The configuration depicted in Figure 2 is essentially a dodecahedron; only the unique distances are shown. The amount of distortion from a regular dodecahedron found in this case is similar to that reported by Pawley<sup>6c</sup> in a recent refinement of  $B_8Cl_8$ . The zinc atom in  $Zn(NH_3)_4B_8H_8$  is tetrahedrally coordinated to four nitrogen atoms with a Zn-N distance of 2.04 Å. More complete structural details on  $Zn(NH_3)_4B_8H_8$  will be reported by one of us (L. G.) later.

In solution the  $B_8H_8^{2-}$  ion exhibits a  $B^{11}$  nmr spectrum which consists of two peaks of separation 128 cps; this doublet is due to boron-hydrogen spin-spin splitting (Figure 3). Consistent with the remarks about  $B_7H_7^{2-}$  in solution these data simply permit the statement that there is a *minimum* of one boron atom environment. There are several ways in which one might rationalize this  $B^{11}$  nmr spectrum. There is, of course, the possibility that the energy level for the  $D_{4d}$  square antiprismatic arrangement has been lowered relative to the  $D_{2d}$  configuration because of solvation effects, *e.g.*, solvation of the square faces, and that all of the boron atoms are environmentally equivalent. Another explanation is a rapid polyhedral rearrangement, rapid relative to the nmr time scale, that would provide for spectroscopic equivalence of boron atoms. It has been conjectured<sup>10a</sup> that the ground-state lifetimes of  $D_{4d}$  or  $D_{2d}$  geometries in metal coordination compounds will be relatively short, since only slight bending modes are required to convert one configuration into the other. A distinctly different

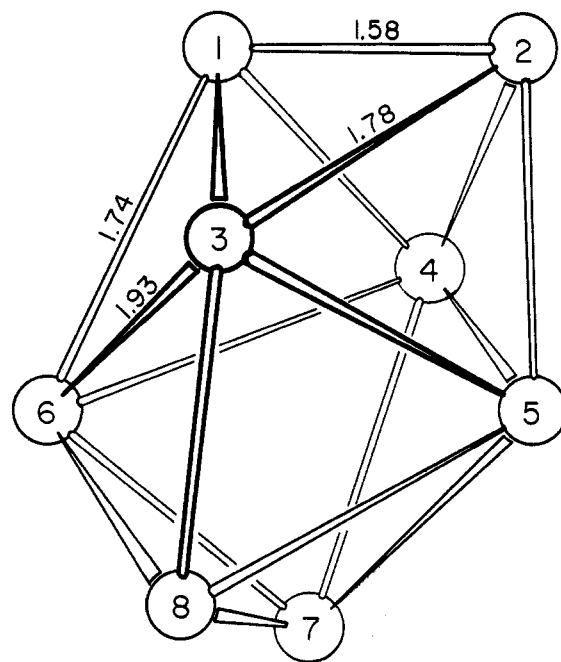


Figure 2.—The molecular configuration of the eight boron atoms in  $Zn(NH_3)_4B_8H_8$ .

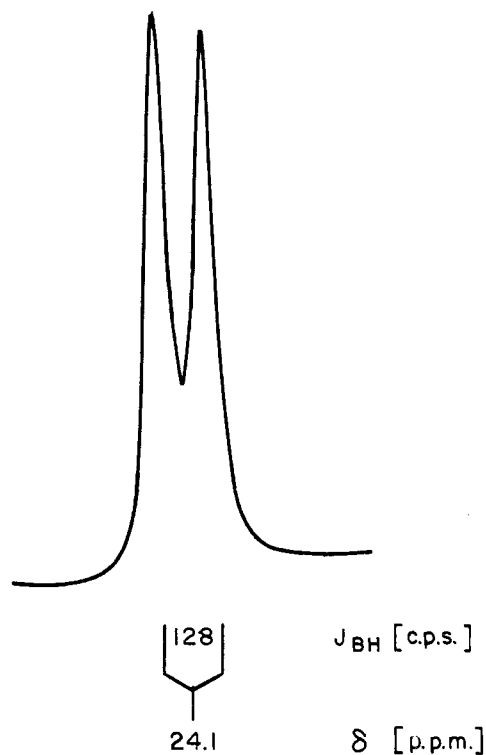


Figure 3.— $B^{11}$  nmr spectrum of  $Cs_2B_8H_8$  in  $H_2O$  at 19.3 Mc; external reference  $B(OCH_3)_3$ .

situation prevails in the polyhedral boranes because the atoms describing the vertices of the polyhedron are in bonding rather than nonbonding interactions. Hence, the barrier to polyhedral rearrangements or intramolecular rearrangements should be at least an order of magnitude higher than in coordination compounds. Furthermore, as we have noted in the  $B_9$  case,<sup>1</sup> the barrier for polyhedral rearrangement is very high, perhaps of the order of magnitude of 30–50 kcal

(10) (a) E. L. Muetterties, *Inorg. Chem.*, **4**, 764 (1965). (b) The appearance of the  $B^{11}$  nmr spectrum of the  $B_{11}H_{11}^{2-}$  ion at 19.3 Mc remains essentially the same in the temperature range from 25 to 150°. This suggests a relatively high barrier to intramolecular polyhedral rearrangement.

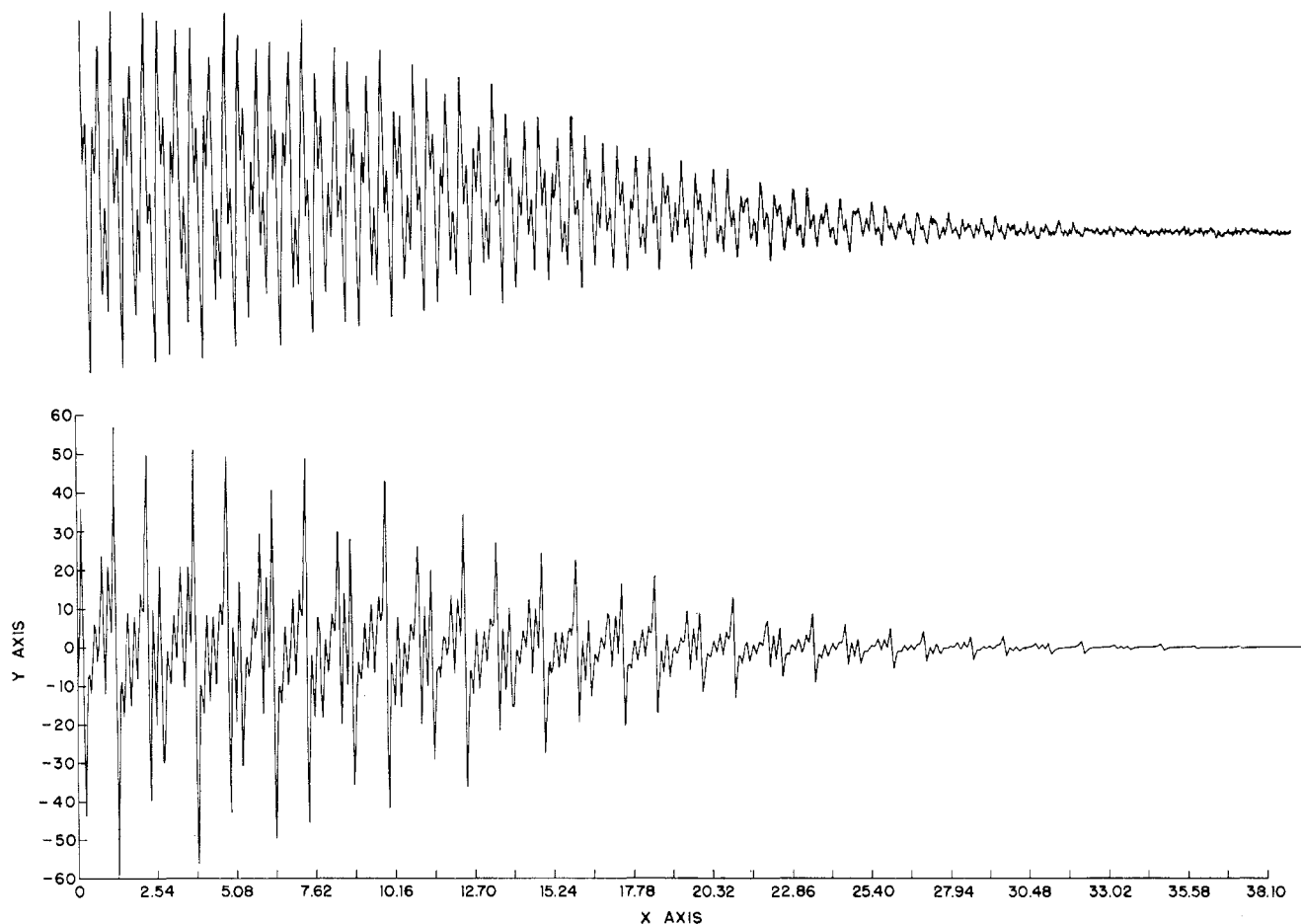


Figure 4.—Esr spectrum ascribed to the  $B_3H_8^-$  ion in tetrahydrofuran: top, observed; bottom, calculated.  $x$  axis scale in gauss.

at  $200^\circ$ .<sup>10b</sup> We do not believe that a rapid polyhedral rearrangement is occurring in the  $B_8$  system. The final rationalization is that the chemical shift between the nonequivalent boron atoms in a  $D_{2d}$  polyhedron (the environmental nonequivalence is relatively small for the relatively large line widths generally encountered in the  $^{11}B$  nmr spectra of boron compounds and especially in polyhedral boranes.<sup>11</sup>

We do not have a strict structural characterization of the  $B_8H_8^-$  radical-ion because of the difficulty of isolating single crystals containing this relatively unstable ion. However, a satisfactory analysis of the complex esr spectrum can be obtained if it is assumed that the ion-radical is a polyhedron with all boron atoms *essentially* equivalent at least on the esr time scale. Small differences in hyperfine coupling constants such as might occur for axial and equatorial

borons cannot be ruled out. This result has important implications with respect to the question of the delocalization of electrons in polyhedral boranes. It does not seem possible to obtain a satisfactory analysis on the basis of a model in which the spin is localized, because such a model would give rise to large differences in the hyperfine coupling constants for different boron and hydrogen atoms.

In Figure 4 the esr spectrum ascribed to the  $B_3H_8^-$  ion in tetrahydrofuran is shown. More than 300 lines can be resolved in this spectrum. The complexity of the spectrum is not surprising. Boron has two naturally occurring isotopes each with a nuclear spin, *i.e.*,  $^{11}B$  spin  $3/2$ , 81.17% abundant, and  $^{10}B$  spin 3, 18.83% abundant. Nine isotopic species differing in the number of  $^{10}B$  atoms incorporated in the molecule must therefore be considered. The relative abundances of these species and the number of esr lines expected from each, assuming all borons and all hydrogens are equivalent, are shown in Table I. As can be seen, the total number of possible lines is very large. However, two factors make an analysis feasible. Firstly, there are only two independent parameters—the hydrogen hyperfine coupling constant and the boron hyperfine coupling constant, since the constants for different isotopes depend only on the magnetic moments and spins of the isotopes and these quantities are known. Secondly, the ratio of the  $^{10}B$  to  $^{11}B$  splittings is for-

(11) Surprisingly, the  $B_8H_8^{2-}$  ion does not seem to follow the empirical rule which says that higher coordination numbers of boron atoms in polyhedral boranes entail higher chemical shifts in the  $^{11}B$  nmr spectra. This empirical concept is obeyed by the ions  $B_7H_7^{2-}$ ,  $B_9H_9^{2-}$ , and  $B_{10}H_{10}^{2-}$ , which all have two sets of nonequivalent boron atoms of coordination number five and six, respectively. The dodecahedral  $B_8H_8^{2-}$  ion also possesses two sets of boron atoms of coordination number five and six, but the environmental differences may be smaller than in the other ions. A difference in coordination number is therefore a necessary but not a sufficient condition for significant differences in chemical shifts between nonequivalent boron atoms. We are at present excluding the  $B_{11}H_{11}^{2-}$  ion from these considerations because its structure has not been established (although  $C_{2v}$  symmetry is likely), and its  $^{11}B$  nmr spectrum at 19.3 Mc is uninterpretable on an *a priori* basis.

TABLE I  
ISOTOPIC SPECIES OF  $B_8H_8^-$

No. of $B^{10}$	Abundance, %	No. of lines
0	18.8444	225
1	34.9708	1386
2	28.3924	2223
3	13.1757	2736
4	3.8203	2925
5	0.7089	2790
6	0.0822	2331
7	0.0054	1548
8	0.0002	441

tuitiously almost an integer (2.9857) so that there will be many near degeneracies in the spectrum.

The analysis of the spectrum was carried out in several stages. Line spectra were first calculated for the simplest isotopic species,  $^{11}B_8H_8$ , using a variety of hyperfine coupling parameters. This eliminated many possibilities and showed, for example, that the correct spread of the spectrum could only be obtained with a large hydrogen coupling constant and a much smaller boron coupling constant. It was also necessary to calculate the relative intensities in the 25-line multiplet arising from eight spins of  $3/2$ . These prove to be 1:8:36:120:322:728:1428:2472:3823:5328:6728:7728:8092. Plausible parameters for this molecule having been found, their veracity was tested by calculating analogous line spectra and intensities for the three other most abundant isotopic species,  $^{11}B_7^{10}BH_8$ ,  $^{11}B_6^{10}B_2H_8$ , and  $^{11}B_5^{10}B_3H_8$ . A set of parameters was found that predicted correct line positions for all these molecules. Line spectra for the complete set of isotopic molecules were then calculated with the aid of a computer. There are many near degeneracies, and the computer was programmed to coalesce all lines within 50-mgauss intervals. Analogous calculations were also carried out for the  $B_7H_7$  and  $B_9H_9$  systems since these also represented chemically conceivable species. Only  $B_8H_8$  gave anything approaching a reasonable fit. Finally Lorentzian lines with several width parameters were constructed at the coalesced line positions and the whole then differentiated to give a simulated spectrum. The spectrum resulting from the parameters  $a_H = 6.10$  gauss,  $a_{11B} = 2.52$  gauss,  $a_{10B} = 0.84$  gauss, and a line width of 100 mgauss is shown in Figure 4. This gives a good fit for line positions and a reasonable, qualitative fit for intensities. In view of the approximations, a better agreement is probably not to be expected. It is considered that this analysis has identified the radical as  $B_8H_8^{\cdot-}$  with a rather high degree of probability.

The analysis above implies that all boron atoms and all hydrogen atoms are equivalent suggesting that the molecular orbital containing the unpaired electron is truly delocalized. It is possible that a fit could also be obtained using a model involving small nonequivalencies, but large differences in the individual boron or hydrogen coupling constants are definitely ruled out. This result provides experimental verification for the concept of "aromatic" structure in boron cage hydrides.

The structure of the  $B_8H_8^{\cdot-}$  ion-radical is not known, but we would tend to favor a  $D_{2d}$  dodecahedral geometry by analogy with  $B_8H_8^{2-}$ . Strictly speaking, for such a  $D_{2d}$  model there are two sets of boron atoms and two sets of hydrogen atoms. However, the differences in environments are not very large and the hyperfine coupling constants may well be very similar. The resolution of the spectrum is insufficient to allow a meaningful test of this possibility. The situation in this respect is analogous to that involving the chemical shifts of  $B_8H_8^{2-}$ . Alternatively, it could be postulated that the two sets of four equivalent boron atoms are exchanging at a rate in excess of  $10^7$  sec. Based on the present knowledge of activation energies for polyhedral rearrangements and of ground-state lifetimes, this does not appear to be a realistic rationalization.

### Theoretical Considerations

**Consideration of Ground-State Geometry in  $B_8H_8^{2-}$  Ion.**—As a continuing effort, we have been attempting to evaluate the utility of LCAO-MO calculations on the polyhedral boranes. A more comprehensive analysis of these approximate calculations will be presented in a forthcoming review.<sup>2b</sup> Of particular interest to us with respect to the  $B_8H_8^{2-}$  ion was the question of effectiveness of theory in identifying the preferred ground-state geometry. The  $B_8$  system is unique because there are at least seven plausible idealized structures for a polyhedron with eight vertices: (1)  $D_{4d}$  square antiprism; (2)  $D_{2d}$  dodecahedron; (3)  $C_{2v}$  square face-bicapped trigonal prism; (4)  $O_h$  cube; (5)  $D_{3h}$  symmetrical bicapped trigonal prism; (6)  $D_{3d}$  symmetrical bicapped trigonal antiprism; (7)  $D_{6h}$  hexagonal bipyramid. All these geometries except the  $D_{3h}$  model (the only geometry for which calculations have been previously presented)<sup>12</sup> have been established for metal coordination polyhedra.<sup>13</sup> In discrete coordination polyhedra the  $D_{4d}$  model is comparable in stability to  $D_{2d}$  and is the more common of the two. The  $D_{3d}$  and the hexagonal bipyramid are found for discrete polyhedra only in actinide chemistry, particularly uranyl, plutonyl, and neptunyl species. The  $C_{2v}$  model, which might be described as a frustrated nine-coordinate model, is found in periodic lattices of actinide and lanthanide complexes. The cube is found in ionic lattices only.

Before making our calculations we had no structural data and entertained the relatively pessimistic view that the molecular orbital calculations probably would not serve even as a *relative* guide to the preferred geometry of  $B_8H_8^{2-}$ . The calculations were carried out using the Hoffman-Lipscomb procedure.

Regular geometries were assumed with B-B and B-H distances of 1.80 and 1.19 Å, respectively. Our basis set in the molecular orbital expansions consisted of 8 hydrogen Slater orbitals, exponent 1.0, and 8 2s

(12) W. N. Lipscomb, "Boron Hydrides," W. A. Benjamin, Inc., New York, N. Y., 1966.

(13) Cf. E. L. Muetterties and C. M. Wright, *Quant. Rev. (London)*, **21**, 109 (1967), for a discussion of these and for references to the original literature.

TABLE II  
 B<sub>8</sub>H<sub>8</sub><sup>2-</sup>—TOTAL ENERGY AND GROSS ATOMIC POPULATIONS

	D <sub>4d</sub>	C <sub>2v</sub>	D <sub>2d</sub>	O <sub>h</sub>	D <sub>3d</sub>	D <sub>3h</sub>
Total energy	-492.689	-490.851	-490.589	-488.893	-488.645	-488.181
Boron population	3.057	3.298 (sq) 3.075 (rhb) 2.793 (rhnb)	3.175 (ax) 2.940 (eq)	3.113	3.446 (ax) 2.949 (eq)	3.105 (ax) 3.076 (eq)
Hydrogen population	1.193	1.136 (sq) 1.171 (rhb) 1.155 (rhnb)	1.180 (ax) 1.205 (eq)	1.137	1.157 (ax) 1.184 (eq)	1.152 (ax) 1.172 (eq)

and 24 2p boron Slater orbitals, exponent 1.3. The  $H_{ii}$  terms were chosen in the conventional way as the valence state ionization potentials with  $H_{ii}(\text{H}1s) = -13.60$  eV,  $H_{ii}(\text{B}2s) = -14.91$  eV,  $H_{ii}(\text{B}2p) = -8.42$  eV. The off-diagonal elements were evaluated using the relationship  $H_{ij} = (k/2)(H_{jj} + H_{ii})S_{ij}$  with  $k = 1.75$  as originally suggested by Helmholtz and Wolfsberg.<sup>14</sup> The results for the total energies were as shown below.

Geometry	Total energies, ev	Geometry	Total energies, ev
D <sub>4d</sub>	-492.69	O <sub>h</sub>	-488.89
C <sub>2v</sub>	-490.85	D <sub>3d</sub>	-488.65
D <sub>2d</sub>	-490.59	D <sub>3h</sub>	-488.18

These results show several interesting features. The expected high-energy models O<sub>h</sub>, D<sub>3d</sub>, and D<sub>3h</sub> were almost uniquely defined as such with about a 4-eV difference from the low-energy D<sub>4d</sub> model. At this point we had preliminary X-ray data that suggested that D<sub>4d</sub> was the polyhedral symmetry in the crystalline state. Less in accord with expectation, however, was the 2-eV separation between the D<sub>4d</sub> and C<sub>2v</sub> models. Although differentiated by symmetry elements these polyhedra are very similar and are probably very readily interconverted by a bending or stretching modes for most coordination compounds.<sup>15-17</sup> Furthermore there is an intuitive preference for the dodecahedral (D<sub>2d</sub>) model since in this polyhedron the boron-boron interactions as well as the average boron coordination number would be maximized. A further argument in favor of D<sub>2d</sub> over D<sub>4d</sub> was the empirical rule that triangular faces prevail in closed boron polyhedral structures. With the final resolution of the crystalline state geometry for the B<sub>8</sub>H<sub>8</sub><sup>2-</sup> ion it was apparent that the approximate theory does not correctly predict the most stable geometry for B<sub>8</sub>H<sub>8</sub><sup>2-</sup> in the solid state. It should be pointed out, however, that the B<sub>8</sub> system is without question one of the more difficult ones. (The seven-atom system is of comparable complexity.) It would be of interest to carry out similar calculations for either the B<sub>6</sub> or B<sub>9</sub> polyhedra since in these cases the octahedron and tricapped trigonal prism, respectively, are expected to be favored over other possible idealized geometries such as the trigonal prism and the monocapped square antiprism. If the theory did not clearly identify these as the most stable species, it could safely

be concluded that the theory in its present form is not as good a guide to preferred ground-state geometries as are intuitive or empirical considerations. For the 12-atom system, the calculations of Hoffmann and Lipscomb do identify the icosahedron as a lower energy species than the cuboctahedron.

The gross atomic populations (Table II) of the various polyhedra prove to be rather uninteresting with the exception of the D<sub>3d</sub> model in which there is a difference of 0.5 in the charge density of the equatorial and apical boron atoms. This represents an improbable charge distribution. The overlap populations between atoms may be taken as a guide to bond strengths and provide rather more insight into the question of relative stabilities of the different geometries. The following generalizations can be made.

(1) In all cases each boron has a bonding interaction with all of its nearest neighbors (Table III) and antibonding interactions with nonnearest neighbors (Table IV).

(2) As the number of nearest neighbors increases, the bond strength to each decreases. This decrease is less than proportional so that there is a net advantage in maximizing the number of nearest neighbors. Thus, the individual boron-boron bonds are stronger in O<sub>h</sub>, which has only three nearest neighbors, than in D<sub>4d</sub> with four or equatorial D<sub>2d</sub> with five. However, the total overlap population of five equatorial D<sub>2d</sub> bonds is greater than the total for four bonds at the axial position. Over-all D<sub>2d</sub> gives the largest total overlap population. Thus, as far as the bonding in the cage is concerned, the favorable geometry is the compact D<sub>2d</sub> followed closely by D<sub>4d</sub>.

(3) The above trend is offset to some extent by the antibonding interactions with nonnearest neighbors which are also at a maximum for compact structures (Table IV). Thus considering only the bonding and antibonding interactions in the boron cage the overlap population analysis suggests the stability order D<sub>2d</sub> > D<sub>4d</sub> > D<sub>3d</sub> > D<sub>3h</sub> > O<sub>h</sub> > C<sub>2v</sub>.

(4) There is, of course, strong B-H bond interaction only with neighboring boron atoms and a general trend that the stronger the B-B bonding, the weaker the B-H bonding. The H antibonding interactions are determined predominantly by the number of next nearest neighbors. Thus in D<sub>4d</sub> there are four next nearest neighbor bonds and an overlap population of -0.2076. In equatorial D<sub>2d</sub> there are five and an overlap population of -0.2676.

Without going through the obvious machinations it

(14) M. Wolfsberg and L. Helmholtz, *J. Chem. Phys.*, **20**, 837 (1952).

(15) J. V. Silverton and J. L. Hoard, *Inorg. Chem.*, **2**, 243 (1963).

(16) E. L. Muetterties and C. M. Wright, *J. Am. Chem. Soc.*, **87**, 4706 (1965).

(17) E. L. Muetterties, *Pure Appl. Chem.*, **10**, 53 (1965).

TABLE III  
 OVERLAP POPULATION ANALYSIS FOR  $B_8H_8^{2-}$ 

		$D_{4d}$	$C_{2v}$ "Square"	$D_{2d}$ "Axial"	$O_h$	$D_{3d}$ "Axial"	$D_{3h}$ "Axial"
Nearest neighbors		{ 0.5652	0.8517	0.7026	0.6389	0.6349	0.6056
		{ 0.5652	0.7291	0.4365	0.6389	0.6349	0.6056
$D_{4d}$	4	{ 0.5136	0.1378	0.4365	0.6389	0.6349	0.6056
		{ 0.5136	0.0880	0.5697			
$C_{2v}$	4.25	2.1576	1.8066	2.1453	1.9167	1.9047	1.8168
$D_{2d}$	4.5						
			"Rhombus bond"	"Equatorial"		"Equatorial"	"Equatorial"
$O_h$	3		0.6865	0.4365		0.6349	0.6056
			0.6865	0.4365		0.2958	0.3773
$D_{3d}$	4.5		0.1378	0.5697		0.2958	0.3773
			0.1378	0.3891		0.4405	0.5409
$D_{3h}$	3.75		0.2665	0.3891		0.4405	
			1.9151	2.2209		2.1075	1.9011
			"Rhombus non"				
			0.6865				
			0.6865				
			0.0880				
			0.0880				
			1.5490				
Weighted mean		2.1576	1.7693	2.1831	1.9167	2.0568	1.8800

 TABLE IV  
 OVERLAP POPULATION ANALYSIS FOR  $B_8H_8^{2-}$ 

	$D_{4d}$	$C_{2v}$ "Square"	$D_{2d}$ "Axial"	$O_h$	$D_{3d}$ "Axial"	$D_{3h}$ "Axial"
Nonneighbor interactions in cage	-0.2947	-0.2065	-0.2967	-0.2372	-0.2588	-0.1853
Net bonding/B in cage	1.8629	1.6001	1.8486	1.6795	1.6459	1.6315
		"Rhombus B"	"Equatorial"		"Equatorial"	"Equatorial"
		-0.1072	-0.3359		-0.2329	-0.0864
		1.8079	1.8850		1.8746	1.8147
		"Rhombus NB"				
		-0.1290				
		1.4200				
Average net bonding in cage	1.8629	1.6070	1.8668	1.6795	1.8174	1.7689

is clear that one can rationalize a ground-state geometry of  $D_{2d}$  symmetry by weighting more heavily the consideration of maximizing boron-boron interactions. However, as noted above this would have been simply the intuitive guiding principle for predicting geometries in this particular system.

Molecular orbital calculations were also performed on a distorted  $D_{2d}$  model. The atom coordinates here were taken from the least-squares refinement of  $Zn(NH_3)_4B_8H_8$ . The calculated total energy for the distorted model was lower than that of the regular model (-491.32 vs. -490.59 eV), but higher than for the  $D_{4d}$  model (-492.69 eV). However, this is of questionable significance since, among other things, the average B-B distance was 0.02 Å shorter in the distorted model. A striking feature of the calculation on the distorted model is that the hydrogen atom environments are noticeably more equivalent. The gross atomic hydrogen populations are now 1.191 (ax) and 1.198 (eq), the boron-hydrogen overlap populations

are 0.8845 (ax) and 0.8855 (eq), and the hydrogen nonbonding overlaps are -0.2219 (ax) and -0.2336 (eq); these values can be compared with the corresponding values for the regular  $D_{2d}$  geometry in Tables II and V.

**Predictions Relating to Oxidative and Reductive Reactions of  $B_8H_8^{2-}$ .**—The energies of the top filled orbitals for the various geometries are quite similar, ranging from -9.16 eV in  $O_h$  symmetry to -9.90 eV in  $D_{4d}$  symmetry. These orbitals are higher in energy than those reported for calculations on other polyhedral boranes. One might therefore predict that the  $B_8H_8^{2-}$  ion would be the most readily oxidized polyhedral ion and this is the case with the exception of  $B_7H_7^{2-}$  which appears to be the most readily degraded polyhedral ion. As noted above,  $B_8H_8^{2-}$  undergoes air oxidation to give first  $B_8H_8 \cdot^-$ , which is then further degraded to  $B_7H_7^{2-}$  and  $B_6H_6^{2-}$ , and ultimately to boric acid and hydrogen.

The energy gap for the highest bonding orbital and

TABLE V  
 OVERLAP POPULATION ANALYSIS FOR  $B_8H_8^{2-}$ 

	$D_{4d}$	$C_{2v}$ "Square"	$D_{2d}$ "Axial"	$O_h$	$D_{3d}$ "Axial"	$D_{5h}$ "Axial"
Boron-hydrogen bonds	0.8838	0.9280	0.8794	0.8459	0.8700	0.8713
Hydrogen nonbonding interactions	-0.2076	-0.1935	-0.1767	-0.1323	-0.1279	-0.1258
Net	0.6762	0.7345	0.7027	0.7136	0.7421	0.7455
		"Rhombus B"	"Equatorial"		"Equatorial"	"Equatorial"
		0.8635	0.8899		0.8738	0.8748
		-0.1846	-0.2676		-0.2333	-0.2321
		0.6789	0.6223		0.6405	0.6427
		"Rhombus NB"				
		0.8710				
		-0.1294				
		0.7461				
Average	0.6762	0.7235	0.6625	0.7136	0.6659	0.6684
Sum B + H	2.5391	2.3305	2.5293	2.3931	2.4833	2.4373
	1	6	2	5	3	4

the lowest empty orbital from our calculations ranges from about 6.02 eV in  $D_{5h}$  symmetry to 8.93 eV in  $C_{2v}$  symmetry. This gap is smaller than that for the other ions. Therefore, one might predict a more facile reduction of  $B_8H_8^{2-}$  ion. However, like all other dinegative ions from  $B_6H_6^{2-}$  to  $B_{12}H_{12}^{2-}$ , the anion  $B_8H_8^{2-}$  is highly resistant to reduction.

**The  $B_8$  Ion-Radical.**—Based on the total energies, the calculations predict  $D_{4d}$  symmetry for the ion-radical. In fact the order for the various geometries parallels that for  $B_8H_8^{2-}$ .

Geometry	Total energy, eV	Geometry	Total energy, eV
$D_{4d}$	-482.79	$O_h$	-479.47
$C_{2v}$	-481.24	$D_{3d}$	-479.29
$D_{2d}$	-481.05	$D_{5h}$	-478.98

We do not believe, however, that these calculations serve as any reasonable guide to preferred ground-state geometries in this  $B_8$  ion-radical system. Based on purely empirical considerations, we would predict as the ground-state geometry of this ion-radical the  $D_{2d}$  dodecahedron or a slightly distorted version of this molecule. It should be noted that if  $D_{4d}$  symmetry prevails, the ion-radical is a Jahn-Teller species subject to distortion. A dynamic effect similar to that postulated for  $C_6H_6^{2-}$  would probably be expected. As noted in the earlier section, the esr analysis indicates that the odd electron in this species is equally coupled with all the boron atoms and with all the hydrogen atoms. This does not necessarily mean that the boron atoms are environmentally exactly equivalent. Quite probably it is simply a case of accidental degeneracies. It is conceivable that the barrier to polyhedral rearrangements between  $D_{4d}$  and  $D_{2d}$  geometries is relatively low and that the esr data reflect an average. However, both in view of the time scale of the esr experiments and previous data for barriers for polyhedral isomerizations, we consider this unlikely.

**The  $B_7H_7^{2-}$  Ion.**—The original calculations by Lipscomb and Hoffmann on the  $B_7$  polyhedron indicate

that the closed shell configuration should be achieved in the dinegative ion, namely,  $B_7H_7^{2-}$ . We have repeated these calculations and reach the same conclusion. As noted in Table VI, there is a fair sized energy gap between the top bonding level and the first empty level.

 TABLE VI  
 $B_7H_7^{2-}$ 

Equatorial B-B, A	Axial B-B, A	Total energy, eV	Energy gap, eV
1.8	1.903	-434.30	5.28
1.8	1.857	-433.40	5.22
1.8	1.8	-431.89	4.64
1.8	1.751	-430.13	4.06
1.8	1.705	-427.97	3.43

We have also performed calculations of the  $B_7$  ion in  $D_{5h}$  symmetry maintaining the equatorial boron-boron distance at 1.8 Å and varying the axial boron-boron bond distance between 1.7 and 1.9 Å. Total energy diminishes with increased axial bond distances, and it appears that a minimum would be reached between 1.9 and 1.95 Å. Deviations from strict  $D_{5h}$  symmetry in a static geometry in which some of the boron atoms in the equatorial plane are displaced toward one axial boron atom and the rest toward the other axial boron atom would tend to increase the total binding energy, a consideration that perhaps argues for a ground-state geometry of something less than  $D_{5h}$  symmetry. In metal coordination compounds at least four idealized geometries have been established or suggested: the  $C_{2v}$  square face-capped trigonal prism, the  $C_{3v}$  monocapped octahedron, the pentagonal bipyramid, and a  $C_2$  model very closely related to the pentagonal bipyramid. This latter structure is illustrated in Figure 5. All these geometries are very closely related,<sup>18,19</sup> and, as has been pointed out before, only a slight bending mode is required for intramolecular re-

(18) E. L. Muetterties, *Inorg. Chem.*, **4**, 769 (1965).

(19) E. L. Muetterties and K. J. Packer, *J. Am. Chem. Soc.*, **86**, 293 (1964).

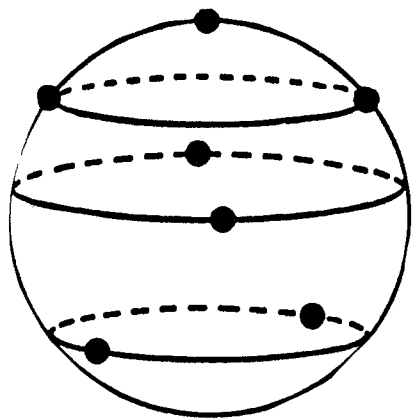


Figure 5.—Possible structure of the  $B_7H_7^{2-}$  ion with  $C_2$  symmetry (spherical representation).

arrangements. The  $^{11}B$  nmr data for  $B_7H_7^{2-}$  establish a minimum of two boron atom environments of relative populations 5 and 2. These data are not consistent with any of the idealized seven-coordinate geometries but the pentagonal bipyramid. However, considering geometries such as the  $C_2$  species and its very close relationship to the pentagonal bipyramid, it is conceivable that, because of the small chemical shifts generally encountered in  $^{11}B$  nmr patterns for polyhedral boranes and the relatively large line widths, a geometry such as the  $C_2$  species could actually prevail as the stable ground-state geometry. Alternatively, the  $B_7H_7^{2-}$  ion could be considered a dynamic case in which  $D_{5h}$  symmetry is the average geometry. The dynamic process could involve a pseudo-rotation-like motion for the five equatorial boron atoms, that is, a constant out-of-phase rise and fall of equatorial boron atoms from the time-averaged equatorial plane.

Unfortunately we have no spectroscopic technique that will provide a *rigorous* definition of the ground-state geometry for  $B_7H_7^{2-}$  in solution. We have recourse to analyses of the geometries in the solid state; however, unless such an analysis shows no significant distortion of any one of the possible idealized geometries for seven-atom polyhedra as well as no significant cation-anion type interactions, it will not be evident whether the observed solid-state structure is dictated by packing forces or is representative for the geometry of an isolated  $B_7H_7^{2-}$  ion.

### Experimental Section

**Preparation of  $Cs_2B_3H_8$ .**—Crude hydrated  $Na_2B_3H_8 \cdot xH_2O$  (4.3 g), prepared as described,<sup>1</sup> was stirred for about 15 min with 150 ml of dimethoxyethane close to the boiling point of the solvent. The mixture was filtered, and the residue was treated with another portion of 100 ml of warm dimethoxyethane. The solution was filtered again, and the two deep-red filtrates were combined. The remaining insoluble fraction was converted to  $Cs_2B_3H_8$  by dissolution in water and precipitation with cesium hydroxide. The recovery of  $Cs_2B_3H_8$  was 1.4 g. A stream of air was then bubbled through the red dimethoxyethane solution for about 2 hr. The red color gradually vanished, and the mixture became milky white. It was then treated with 100 ml of 0.5 *N* cesium hydroxide solution, and the resulting precipitate was recrystallized from 90 ml of water to give 3.2 g of  $Cs_2B_3H_8$  as white crystals.

*Anal.* Calcd for  $Cs_2B_3H_8$ : B, 24.0; H, 2.2; hydrolytic  $H_2$ ,

1057 ml/g. Found: B, 24.2; H, 2.5; hydrolytic  $H_2$ , 1059 ml/g; density (by flotation),  $2.34 \pm 0.01$  cm<sup>3</sup>/g.

**Preparation of Other Salts of  $B_3H_3^{2-}$ .**—The hydrated sodium salt of  $B_3H_3^{2-}$  was prepared by passing a solution of  $Cs_2B_3H_8$  through a sodium ion-exchange column and evaporating the effluent to dryness. Aqueous or ammoniacal solutions of the sodium salt were used to prepare the other salts described below by metathesis with soluble salts of the respective cations. The rubidium salt was recrystallized from water, and the metal ammine salts were recrystallized from dilute ammonium hydroxide. Owing to low solubility in ammonium hydroxide solution and unfavorable temperature coefficients, the purification of metal ammine salts of  $B_3H_3^{2-}$  by recrystallization proved troublesome and recovery of pure material was generally poor.

*Anal.* Calcd for  $Rb_2B_3H_8$ : B, 32.6; H, 3.0; hydrolytic  $H_2$ , 1434 ml/g. Found: B, 32.5; H, 3.3; hydrolytic  $H_2$ , 1450 ml/g.

*Anal.* Calcd for  $Zn(NH_3)_4B_3H_8$ : N, 24.6; H, 8.8. Found: N, 24.2; H, 9.1.

*Anal.* Calcd for  $Cd(NH_3)_2B_3H_8 \cdot 0.5H_2O$ : B, 34.6; N, 11.2; H, 6.1. Found: B, 34.5; N, 12.0; H, 6.4.

Crystals of  $Cd(NH_3)_2B_3H_8 \cdot 0.5H_2O$  (colorless glittering prisms) are monoclinic with the parameters  $a = 6.387$  Å,  $b = 13.084$  Å,  $c = 14.242$  Å,  $\beta = 124.0^\circ$ ,  $Z = 4$ . The calculated density was  $\rho_x = 1.68$  and the experimentally determined density was  $\rho_E = 1.65$ .

**$[(C_6H_5)_3PCH_3]_2B_3H_8$  and  $[(C_6H_5)_3PCH_3]B_3H_8$ .**—When an aqueous solution of triphenylmethylphosphonium bromide was added to an aqueous solution of  $Na_2B_3H_8$ , a brick-red solid precipitated which displayed a broad unresolved esr signal. It decomposed without melting at  $216^\circ$  and was sparingly soluble in acetone and dimethoxyethane giving orange, unstable solutions.

*Anal.* Calcd for  $[(C_6H_5)_3PCH_3]_2B_3H_8$ : C, 70.3; H, 6.8; P, 9.5; B, 13.3. Found: C, 69.5; H, 7.2; P, 9.3; B, 14.5.

It was estimated from the intensity of the esr signal that about 1–2% of the material was the  $B_3H_3^-$  salt,  $[(C_6H_5)_3PCH_3]B_3H_8$ , the remainder being  $[(C_6H_5)_3PCH_3]_2B_3H_8$  as confirmed by the analytical data. Similarly, the bis-tetrabutylammonium salt of  $B_3H_3^{2-}$ , colorless immediately after preparation, is oxidized readily to the red  $B_3H_3^-$  salt when solutions of  $[(C_4H_9)_4N]_2B_3H_8$  in dimethyl sulfoxide, acetonitrile, chloroform, and even water are exposed to air.

**Spectral Data of  $B_3H_3^{2-}$ .**—The infrared spectrum of  $Rb_2B_3H_8$  in aqueous solution showed two strong bands at 2455 and 2430  $cm^{-1}$  in the B–H stretching region. A Nujol mull of  $Rb_2B_3H_8$ , recorded on a Perkin-Elmer grating instrument, showed the following bands: 2480 (vs), 2450 (vs), 1138 (m), 1000 (vw), 950 (vw), 900 (w), 860 (w), 834 (vw), 715 (vw), 660 (vw), 630 (w), and 620 (w)  $cm^{-1}$ .

**Bromination of  $B_3H_3^{2-}$ .**—Sodium hypobromite solution was added to a solution of 0.4 g of  $Rb_2B_3H_8$  in 20 ml of 2 *N* sodium hydroxide solution until the yellow color of the solution persisted. The mixture was heated to  $90^\circ$  for about 10 min, the warm solution was filtered, and tetramethylammonium chloride was added to the filtrate. The crude white precipitate was first recrystallized from 20 ml of a dimethoxyethane (80%) and water (20%) mixture, and then from a mixture of dimethoxyethane and concentrated hydrochloric acid in about the same proportions. The recovery was 0.3 g of  $[(CH_3)_4N]_2B_3Br_3H_2$ , decomposing at  $380^\circ$ .

*Anal.* Calcd for  $[(CH_3)_4N]_2B_3Br_3H_2$ : C, 23.1; H, 5.1; N, 3.4; B, 10.5; Br, 57.9. Found: C, 22.4; H, 5.1; N, 3.4; B, 10.6; Br, 59.4.

The infrared spectrum showed weak B–H absorption at 2500  $cm^{-1}$ ; other bands not due to the cation were at 1100, 920, and 895  $cm^{-1}$ . The ultraviolet spectrum in acetonitrile showed absorption at 3170 Å ( $\epsilon$  145) and at 2200 Å ( $\epsilon$  8000). The  $^{11}B$  nmr spectrum consisted of a broad peak at  $\delta +17.5$  ppm [reference  $(CH_3O)_3B$ ] which tailed into another much less intense peak at  $\delta +41.2$  ppm.

**Polarographic Data.**—Table VII summarizes results of a polarographic examination of the three ions  $B_3H_3^{2-}$ ,  $B_3H_3^-$ , and  $B_3H_6^{2-}$ . They were obtained in 0.5 *M* aqueous  $K_2SO_4$  solution

TABLE VII

Compd	$c, M$	$i_0,$ amp/cm <sup>2</sup>	$E_{1/2}, v$
Cs <sub>2</sub> B <sub>6</sub> H <sub>8</sub>	$1.90 \times 10^{-3}$	$2.9 \times 10^{-3}$	-0.33
Cs <sub>2</sub> B <sub>8</sub> H <sub>8</sub>	$1.87 \times 10^{-3}$	$2.9 \times 10^{-3}$	-0.04
Rb <sub>2</sub> B <sub>6</sub> H <sub>9</sub>	$2.80 \times 10^{-3}$	$2.5 \times 10^{-4}$	-0.15
Rb <sub>2</sub> B <sub>9</sub> H <sub>9</sub>		$3.7 \times 10^{-3}^a$	$\pm 0.00$

<sup>a</sup> Extrapolated value.

using a platinum electrode *vs.* a saturated calomel electrode. The electrochemical processes were all diffusion controlled at the platinum surface. The half-wave potentials were deliberately measured at approximately equal concentrations of the respective salts and about equal current densities, because the potential

that the oxidative stability of B<sub>11</sub>H<sub>11</sub><sup>2-</sup> is intermediate between that of B<sub>10</sub>H<sub>10</sub><sup>2-</sup> and B<sub>9</sub>H<sub>9</sub><sup>2-</sup>.

**Preparation of Salts of B<sub>7</sub>H<sub>7</sub><sup>2-</sup>. Method A.**—The filtrate from the crude Cs<sub>2</sub>B<sub>6</sub>H<sub>8</sub> isolation step described above assumed a transient pink color. A small amount of Cs<sub>2</sub>B<sub>6</sub>H<sub>8</sub> precipitated when the solution stood exposed to air for several hours. The yield of Cs<sub>2</sub>B<sub>6</sub>H<sub>8</sub>, after recrystallization of the crude salt from water, was 30 mg.

*Anal.* Calcd for Cs<sub>2</sub>B<sub>6</sub>H<sub>8</sub>: B, 19.3; H, 1.8. Found: B, 19.2; H, 2.2.

The infrared spectrum was identical with that of an authentic sample. The <sup>11</sup>B nmr spectrum showed a doublet at  $\delta +31.7$  ppm, with  $J_{BH} = 122$  cps. The reported<sup>8</sup> chemical shift for B<sub>6</sub>H<sub>6</sub><sup>2-</sup> is  $\delta +31.1$  ppm. The filtrate from the crude Cs<sub>2</sub>B<sub>6</sub>H<sub>8</sub>

TABLE VIII  
HÜCKEL ENERGIES FOR B<sub>8</sub>H<sub>8</sub><sup>2-</sup>

	D <sub>2d</sub> sym	C <sub>2v</sub> sym	D <sub>4d</sub> sym	O <sub>h</sub> sym	D <sub>3h</sub> sym	D <sub>3d</sub> sym
1	63.959878	53.461821	57.944374	90.650451	58.964901	53.326494
2	47.378995	42.899726	57.943752	45.158722	58.963410	52.907982
3	42.016765	42.162763	39.929639	45.158714	40.418795	52.905884
4	42.016762	37.687834	39.929634	45.157129	39.798921	40.703276
5	37.412932	34.261899	39.006852	26.648381	31.388921	32.443594
6	35.623010	33.635902	32.946437	26.647595	28.246669	32.441872
7	35.623004	32.804033	32.946426	26.647594	28.246061	28.960702
8	24.330600	29.368214	23.397116	25.814092	25.084803	25.046051
9	22.907333	23.882969	23.394227	19.252379	25.084537	25.045127
10	22.333723	18.523224	21.552863	19.252272	23.176191	22.963776
11	22.333719	15.979096	21.552861	19.252269	21.686728	19.906907
12	13.915168	12.002770	16.936114	17.384275	17.929677	19.796211
13	13.341128	9.551937	12.163664	5.161037	17.929272	19.795881
14	13.341126	9.438441	8.238291	5.160939	10.226835	13.038081
15	10.250081	2.946735	8.238289	4.554638	7.211367	5.654879
16	5.936037	1.743706	7.242728	4.554452	7.211348	4.602499
17	5.936035	-4.590710	2.391840	4.554451	0.492166	4.602100
18	3.939994	-4.657202	2.391840	0.660940	-0.163448	2.625190
19	-0.378181	-5.367960	-0.057304	0.660940	-3.614633	1.275068
20	-1.485854	-5.542809	-0.057429	0.660789	-4.869140	1.274863
21	-2.382412	-7.052529	-0.390454	-8.592178	-4.869193	-4.530307
22	-2.382413	-8.068168	-7.188153	-8.592216	-6.023940	-6.317998
23	-7.156047	-8.929336	-7.188154	-8.592218	-6.024020	-6.318099
24	-9.428439	-9.543102	-9.901238	-9.165166	-9.613742	-9.363149
25	-10.268324	-9.988744	-9.901239	-9.165193	-9.613748	-9.363185
26	-10.268325	-10.406116	-10.919740	-9.165195	-10.001089	-10.701800
27	-10.978463	-10.424248	-10.919754	-11.297381	-10.001121	-10.701898
28	-11.005545	-10.556127	-10.953754	-11.297396	-11.334684	-11.124901
29	-11.602249	-10.883685	-11.791587	-12.048372	-11.334698	-11.124971
30	-11.602255	-11.783935	-12.056604	-12.048373	-12.048491	-11.719991
31	-12.652437	-13.179114	-12.056606	-12.048384	-12.559791	-12.808932
32	-13.891886	-13.386146	-14.048388	-14.011484	-13.974244	-13.946635
33	-16.043063	-16.071285	-15.956941	-15.125174	-15.692793	-15.426217
34	-16.079650	-16.119248	-15.956992	-16.558304	-15.711446	-15.907859
35	-16.100270	-16.693559	-16.245951	-16.558306	-15.711463	-15.907924
36	-16.100270	-17.109747	-16.245954	-16.558372	-17.171803	-17.250655
37	-18.478978	-18.263955	-18.199894	-19.008538	-18.254601	-18.190551
38	-18.478987	-18.862732	-19.267990	-19.008602	-18.254634	-18.190572
39	-19.500263	-20.217609	-19.267991	-19.008607	-20.320821	-19.815806
40	-22.815301	-21.936271	-22.654132	-22.373908	-22.491176	-22.777668

may be subject to variations as a function of these variables in systems which do not obey the Nernst equation. It may be noted that the potentials for the three ions listed, while comparable among each other, are not *directly* comparable to the oxidation potentials reported previously<sup>1,20</sup> for B<sub>11</sub>H<sub>11</sub><sup>2-</sup>, B<sub>10</sub>H<sub>10</sub><sup>2-</sup>, and B<sub>12</sub>H<sub>12</sub><sup>2-</sup> which were measured under different conditions. Possible minor variations in the numerical values of the potentials will have no bearing, however, on the fact that especially B<sub>10</sub>H<sub>10</sub><sup>2-</sup> and B<sub>12</sub>H<sub>12</sub><sup>2-</sup> are oxidized at much more positive potentials, and

isolation step was then concentrated on the rotating evaporator to a volume of about 20 ml. At this point a yellowish solid separated (250 mg) which consisted of a mixture of cesium salts of the ions B<sub>6</sub>H<sub>6</sub><sup>2-</sup>, B<sub>10</sub>H<sub>10</sub><sup>2-</sup>, and B<sub>7</sub>H<sub>7</sub><sup>2-</sup> as indicated by the <sup>11</sup>B nmr spectrum of the mixture in aqueous solution. This solid was removed by filtration. The remaining filtrate was further concentrated to a volume of about 5 ml. Addition of methanol (about 20 ml) and some diethyl ether caused the precipitation of 100 mg of another yellowish solid which decomposed slowly in aqueous solution. The <sup>11</sup>B nmr spectrum of this solid at 19.2 Mc, run immediately after its preparation, showed two doublets at  $\delta +18.3$  ppm with  $J_{BH} = 119 \pm 4$  cps and at  $\delta +40.7$  ppm

(20) E. L. Muetterties, J. H. Balthis, Y. T. Chia, W. H. Knoth, and H. C. Miller, *Inorg. Chem.*, **3**, 444 (1964).

with  $J_{\text{BH}} = 120 \pm 5$  cps (see Figure 1). The ratio of the relative intensities of the two doublets was 4.90:2 (average of seven individual traces). The sample was free of other boron-containing species detectable by nmr spectroscopy in solution, but it was not possible to reisolate the solid salt from the solution totally free of some borate impurity. However, the analysis obtained is in reasonable agreement with the composition  $\text{Cs}_2\text{B}_7\text{H}_7$ .

*Anal.* Calcd for  $\text{Cs}_2\text{B}_7\text{H}_7$ : B, 21.7. Found: B, 20.4.

**Method B.**—Hydrated  $\text{Na}_2\text{B}_5\text{H}_5 \cdot x\text{H}_2\text{O}$  (2.6 g) was stirred with 300 ml of 1,2-dimethoxyethane at 50–60° for about 10 min. Insoluble material was collected by filtration and converted to  $\text{Cs}_2\text{B}_8\text{H}_8$  by dissolution in water and precipitation with cesium hydroxide. A total of 1.3 g of pure  $\text{Cs}_2\text{B}_8\text{H}_8$  was recovered. The dark red, almost black, dimethoxyethane filtrate was then saturated with a stream of air for about 2 hr, after which time the color of the mixture had changed to milky white. The addition of 100 ml of 1 N cesium hydroxide solution to this mixture precipitated 0.5 g of undegraded  $\text{Cs}_2\text{B}_8\text{H}_8$  which was collected by filtration. Methanol (25 ml) was then added to the filtrate, and the resulting mixture was left standing for 24 hr. A total of 0.8 g of  $\text{Cs}_2\text{B}_8\text{H}_8$  precipitated from the solution during this time. This crude fraction of  $\text{Cs}_2\text{B}_8\text{H}_8$  was contaminated by a small amount of  $\text{Cs}_2\text{B}_{10}\text{H}_{10}$  as indicated by its infrared spectrum, but was obtained pure by two subsequent recrystallizations from 20 ml of water. The yield of pure  $\text{Cs}_2\text{B}_8\text{H}_8$  was 0.6 g. The aqueous dimethoxyethane filtrate from the crude  $\text{Cs}_2\text{B}_8\text{H}_8$  isola-

tion step was then reduced to a volume of about 5 ml on the rotating evaporator at about 10 mm pressure. At this point, 0.3 g of solid precipitated which consisted largely of a mixture of  $\text{Cs}_2\text{B}_{10}\text{H}_{10}$  and  $\text{Cs}_2\text{B}_{12}\text{H}_{12} \cdot \text{CsBH}_4$ . These species were identified by comparing the infrared spectrum of the mixture with spectra of authentic species. This solid was filtered off from the solution, and 10 ml of methanol was added to the filtrate. A white solid (1.5 g) precipitated, the infrared spectrum of which showed the characteristic features of the anion  $\text{B}_7\text{H}_7^{2-}$ . Purification was effected by allowing an aqueous solution of the crude cesium salt to react with an excess of an ammoniacal solution of zinc chloride and recrystallizing the resulting precipitate twice from 30 ml of dilute ammonium hydroxide solution. The final yield was 150 mg of colorless microcrystals of  $[\text{Zn}(\text{NH}_3)_{2.76}(\text{H}_2\text{O})_{1.24}]\text{B}_7\text{H}_7$ . Another less pure crop (0.2 g) was isolated from the mother liquor.

*Anal.* Calcd for  $[\text{Zn}(\text{NH}_3)_{2.76}(\text{H}_2\text{O})_{1.24}]\text{B}_7\text{H}_7$ : Zn, 30.1; N, 17.8; H, 8.2; B, 34.9. Found: Zn, 30.1; N, 17.1; H, 8.3; B, 35.2.

The infrared spectrum of this salt (Nujol mull; cation absorption omitted) showed two strong sharp bands at 2500 and 2450  $\text{cm}^{-1}$  in the B–H stretching region; other absorption occurred at 1100 (m), 1040 (w), and at 920 (m)  $\text{cm}^{-1}$ . The spectrum of  $\text{Cs}_2\text{B}_7\text{H}_7$  was similar; it had an additional band at 720  $\text{cm}^{-1}$  which was masked by  $\text{NH}_3$  absorption in the zinc ammine salt. The ultraviolet spectrum of an aqueous solution of  $\text{Cs}_2\text{B}_7\text{H}_7$  cuts off at 2000 Å.

CONTRIBUTION FROM THE CHEMISTRY DEPARTMENT,  
BROOKHAVEN NATIONAL LABORATORY, UPTON, NEW YORK 11973

## The Crystal and Molecular Structure of Monoiododecaborane<sup>1a</sup>

By A. SEQUEIRA<sup>1b</sup> AND WALTER C. HAMILTON

Received February 22, 1967

The crystal and molecular structure of the low-melting isomer of monoiododecaborane (mp 98.5–100°) has been determined using three-dimensional X-ray diffraction data. The material crystallizes in space group  $P2_1/c$  ( $C_{2h}^5$ ) of the monoclinic system, with eight molecules in a unit cell of dimensions  $a = 13.98$  ( $\sigma = 0.02$ ),  $b = 12.11$  ( $\sigma = 0.02$ ),  $c = 14.34$  Å ( $\sigma = 0.02$ );  $\beta = 120.6^\circ$  ( $\sigma = 0.4$ ). Iodine is at the 1 position in both of the molecules of the asymmetric unit. The structure consists of decaborane-like polyhedral cages that fall in sheets which are roughly parallel to the (120) plane and are held together by the van der Waals interactions between the protruding iodines, as well as by the iodine–hydrogen interactions. The mean B–I bond length is 2.17 Å ( $\sigma = 0.013$ ), and the B–B bond distances are in good agreement with those found in decaborane and in 1-ethyldecaborane.

### Introduction

The iodination of decaborane is known to result in two isomers of monosubstituted and two of the disubstituted derivatives.<sup>2a</sup> Of these, one of the diiodo derivatives has been shown to be substituted in the 2 and 4 positions, based on a determination<sup>2b</sup> of the intramolecular I···I distance from a two-dimensional X-ray diffraction study. Based on this result, the  $\text{B}^{11}$  nmr spectra of the two isomers of  $\text{B}_{10}\text{H}_{13}\text{I}$  have been interpreted by Schaeffer, *et al.*,<sup>3</sup> to show that the substitution occurs at the 2 position in the higher melting

isomer (mp 119), but not in the lower melting isomer (mp 100°). Their interpretations regarding the exact position of substitution in this lower melting isomer have been varied enough to include the 5, 7, 8, 10, the 1,3, or the 6,9 positions.<sup>4</sup> However, the deuterium tracer studies of Hillman<sup>2a,5</sup> favored the 5 substitution. In addition, high-resolution  $\text{B}^{11}$  nmr spectra have been interpreted<sup>6</sup> to show that the substitution occurs at the 1,3 or the 6,9 positions, but any further choice between these two sets could not be made, due to the overlap of 1,3 and 6,9 doublets in the spectra. Hence, an X-ray diffraction study seemed to be appropriate.

(1) (a) Research performed under the auspices of the U. S. Atomic Energy Commission; (b) on deputation from the Atomic Energy Establishment, Trombay, Bombay, India.

(2) (a) M. Hillman, *J. Am. Chem. Soc.*, **82**, 1096 (1960); (b) R. Schaeffer, *ibid.*, **79**, 2726 (1957).

(3) R. Schaeffer, J. N. Shoolery, and R. Jones, *ibid.*, **80**, 2670 (1958).

(4) In particular, see footnote 10 of ref. 3.

(5) After the completion of this work, the deuterium tracer studies of Hillman have been shown to be consistent with the 1 substitution: R. L. Williams, private communication.

(6) R. E. Williams and T. P. Onak, *J. Am. Chem. Soc.*, **86**, 3159 (1964).